Study of Xenon Wall Accommodation Model and Background Flow during Hall Thruster Ground Test

IEPC-2019-235

Presented at the 36th International Electric Propulsion Conference
University of Vienna • Vienna, Austria
September 15-20, 2019

Gen Ito[1,2]
The University of Tokyo, Hongo, Tokyo, 113-8654, Japan
IHI Corporation, Yokohama, Kanagawa, 235-8501, Japan

Rei Kawashima[3] and Kimiya Komurasaki[4]
The University of Tokyo, Hongo, Tokyo, 113-8654, Japan

and

Hiroyuki Koizumi[5]
The University of Tokyo, Hongo, Tokyo, 113-8654, Japan

Abstract: **In 1kW-class SPT-type Hall thruster operation test conducted in Ø 2.0 × 3.0 m vacuum chamber at IHI, it was confirmed that the discharge current and thrust are linearly related to facility background pressure. The one-dimensional model is adopted to calculate the ingestion mass flow rate but the calculated value is much smaller than the experimentally estimated value. To improve this 1D model, the wall accommodation of xenon ion was studied. The molecular dynamics simulation to calculate the trajectory of reflected xenon on solid material was developed and validated by sputtering yield calculation. Simulation results imply that the wall accommodation model of xenon ion with 300 eV is different from complete diffusion and it generates directional reflection. The calculated wall accommodation model of xenon ion bombardment is implemented to the Direct Simulation Monte-Carlo (DSMC) code to calculate the background flux during Hall thruster operation. DSMC simulation shows that the mean flow velocity become negligible when the pumps are located only in downstream of the chamber. Although kinetic energy of reflected propellants in initial reflection takes around 4eV which is higher than thermalized energy, that particles experience multiple wall collision and then the kinetic energy is lost. On the other hand, when the pumps are located on upstream of the chamber, simulation result shows faster mean flow velocity. Ion wall accommodation model becomes more effective to the background flow velocity under the condition that the reflected propellant reaches to the Hall thruster without multiple wall collision.**

Nomenclature

A_{ing} = ingestion area where background neutrals are ingested and ionized by Hall thruster
e = electron charge

[1] Doctoral student, Department of Aeronautics and Astronautics, g.ito@al.t.u-tokyo.ac.jp
[2] Researcher, Technology Platform Center, ito4517@ihi-g.com
[3] Research Associate, Department of Aeronautics and Astronautics, kawashima@al.t.u-tokyo.ac.jp
[4] Professor, Department of Aeronautics and Astronautics, komurasaki@al.t.u-tokyo.ac.jp
[5] Associate Professor, Department of Advanced Energy, koizumi@al.t.u-tokyo.ac.jp

E = potential energy
F_{ing} = ingestion flux
F_{th} = thermal flux
g = relative velocity
I_{corr} = vacuum-corrected discharge current
I_d = discharge current of Hall thruster
I_{ing} = ingestion current
k = Boltzmann constant
m = atomic mass
n_b = number density of background particle
P = pressure
r = distance of atoms
$S(r)$ = switching function of pair potential
Z = nuclear charge
ϵ_0 = electrical permittivity of a vacuum
ρ = atomic electron density
σ = collision cross-section
$\phi(r)$ = pair potential between distance r
i,j = atom index
α,β = type of atom

I.Introduction

HALL thruster is a type of electric propulsion with a simple structure and a relatively wide operating range. In recent years, to meet the demand of various satellites, hall thrusters with several hundred W to several tens of kW power class have been developed[1,2]. The performance of hall thruster is known to depend on the pressure of a ground vacuum facility[3,4]. Particles remaining in vacuum facilities are considered as the cause of the performance change, and this phenomenon is called as background pressure effect. Re-ionization and acceleration of background neutral (this is called as ingestion) contributes to the performance change. However, simple ingestion and ionization of the background gases which randomly move with thermal velocity has been determined to be an inadequate explanation of increased thrust and discharge current.

A measured pressure with installing the collection surface of the ionization gauge in the vacuum chamber in a direction to face the same beam target is 70% lower than that to face to the horizontal with rotated 90 degrees therefrom[5]. This suggests that there is a flow of background gas flowing back toward the beam target thruster. If approximately 70% of the total pressure of the background gas is to be dynamic, it corresponds to the flow with Mach 1.4. Assuming isentropic flow, the velocity of the background flow in the conditions of an average temperature 300 K is estimated to approximately 300 m/s. However, the detail of the background flow has not been studied well. In one-dimensional background flow model developed by Cai et al[6], even in the simple assumption that the ion beam is 100% thermalized, depending on the pumping speed and the arrangement configuration of the pumps, background flow with 100 m/s can be generated. In order to generate flow velocities of 300 m/s, it is necessary to maintain approximately 1 to 2% of the ion beam velocity even if the ion beam of the Hall thruster operating at the discharge voltage of 300 V collides with the chamber wall several times. This implies that the energy of ions is not completely accommodated to the wall. However, the relationship between the wall accommodation model and mean background flow velocity has not been revealed yet. The lack of knowledge about the wall accommodation model of energetic ion makes it difficult.

This paper presents the facility background pressure test results for the 1.0-kW-class high-specific impulse magnetic-layer-type Hall thruster. We applied the one-dimensional background flow model to estimate the background flow during the Hall thruster operation test. It is realized that without upstream pumps in chamber, directional background flow toward the Hall thruster is not able to be generated by one-dimensional model. In order to investigate the detailed background flow property, Direct Simulation Monte-Carlo (DSMC) program has been used in our previous study. Here the wall accommodation model is a simulation parameter and choice of the model affects the simulation results. To overcome this problem, we develop the realistic accommodation model by conducting molecular dynamic simulation. By implementing developed accommodation model to DSMC, the study of the relationship between wall accommodation model and background flow property was conducted.

II.Experiment of background pressure effect and evaluation of ingestion mass flow rate

A. Experimental Apparatus

IHD-1000 thruster is a 1.0-kW-class high-specific impulse magnetic-layer-type Hall thruster manufactured by IHI Corporation, Japan[7]. The thruster is operated by xenon propellant, has two boron-nitride wall rings, and employs magnetic-field topology trimmed by screen yoke. The target operation range of the thruster is 0.5–2 kW in power and 1500–3000 s in specific impulse. A commercial dispenser hollow cathode (HCN-252, Veeco) was mounted externally. In this experiment, thruster operation was performed with discharge voltage of 300 V and propellant flow rate of 20 sccm as nominal conditions. The magnetic field was set with coil currents that minimizes the discharge current oscillation under the condition that the external coil current and the internal coil current are kept at 1: 1. The operation test was conducted in Ø 2.0 × 3.0 m vacuum chamber at IHI. The chamber inside was evacuated by two cryopumps in which the diameter is 30 inch. The flat beam target covered by carbon sheet was installed to the downstream wall.

B. Thrust stand

The thruster was mounted on a pendulum thrust stand inside the vacuum chamber. The position of the thrust stand was then detected by a force sensor. Thrust calibration was conducted with using five weights and pulley arrangement that can apply a known force to the thrust stand under vacuum environment. The power cables were fed from the vacuum feedthroughs to the thruster using a "waterfall" configuration to minimize the thermal drift of the thrust stand readings.

C. Facility Background Pressure Test Results and Discussion

The Figure 1 shows the thrust and discharge current vs. chamber pressure. The linear relationship between those measurements and chamber pressure was observed to be similar to the other reports. In order to evaluate the background pressure effect on thruster performance, the ingestion flux due to facility neutral gas needed to be quantified. The vacuum-corrected discharge current, I_{corr}, was calculated by subtracting the ingestion current from the measured discharge current using

$$I_{corr} = I_d - I_{ing}. \tag{1}$$

When the neutrals are assumed to be singly ionized, the ingestion current is converted to ingestion flux by

$$F_{ing} = \frac{I_{ing}}{eA_{ing}}, \tag{2}$$

where A_{ing} is the area over which the ingestion occurs. Here, by using the discharge channel exit plan as A_{ing}, the ingestion flux without increasing the pressure is calculated as $1.74 \times 10^{20}\ /s/m^2$. If the background flow is considered to be completely thermalized with room temperature T (assumed to be 300 K here), ingestion flux is given by thermal flux calculated by the kinetic approximation

$$F_{th} = \frac{1}{4} n_b \left(\frac{8kT}{\pi m}\right) = \frac{P}{(2\pi kT)^{1/2}}, \tag{3}$$

where n_b is the background gas number density, m is the background gas molecular mass and P is the background gas pressure. By using pressure without increasing additionally, the thermal flux is calculated as $3.66 \times 10^{20}\ /s/m^2$. The ingestion flux estimated by ingestion current is 4.8 times greater than the thermal flux. This implies that the background flow has more than thermal velocity is generated in this experiment.

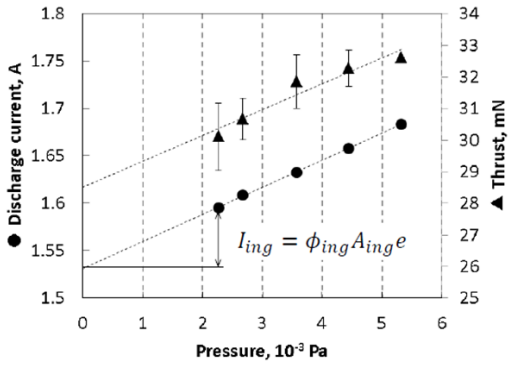

Figure 1. Discharge current (left) and Thrust (right) of IHD-1000 with different background pressure.
The background pressure was controlled by additional xenon flow.

D. One-dimensional background flow model analysis

We applied the background flow model which has been developed by Cai and Frieman to simulate the ingestion mass flow rate[6,8]. This model is the gas-kinetic model based on following assumptions.

Firstly, the rarefied gas is considered a free molecular flow environment. Inter-particle collisions are negligible, which is confirmed by the fact that the Knudsen number is of order unity, which is in the range characteristic of molecular flow.

Secondly, the flow is one-dimensional, in the axis of the thruster. This assumption is consistent with previous studies into background neutral flows, which have yielded good agreement with more complex numerical simulations and empirical measurements[8].

The third assumption is thermodynamic equilibrium flow. Every quantity we compute is at a steady state. This is a validated assumption as the physical variables we compute are typically mean values acquired on the timescale of seconds or minutes, and not on the oscillation characteristics of Hall thrusters that occur at characteristic frequencies on the order of 20 kHz.

When not specified, the wall temperature is set to 300 K and the cryopumps temperature set to 15 K. A sticking coefficient of 0.55 is assumed for the cryopumps. This last value was confirmed in our previous study[9].

The ingestion mass flow rates during the above experiment are calculated by this one-dimensional model and shown in Fig. The geometrical parameters of test facility at IHI given in section II-A are used for the model calculation. The calculated ingestion mass flow rates for different pressure conditions are very close to the values calculated by thermal flux model given by Eq.3. This is explained by the pump location. Since the pump location is the only key element to determine the flow direction, it is impossible to be generated the background flow toward to the thruster with only downstream pump.

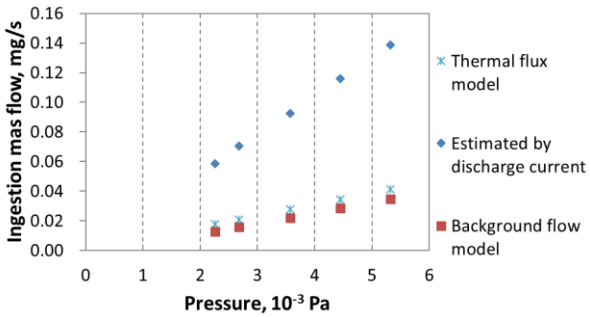

Figure 2. Ingestion mass flow rate of IHD-1000 experiment and background flow model simulation.

III.Molecular dynamics simulation

A. Simulation target and structure

Recently increasing computational power and high-level interatomic potentials have allowed atomistic simulations such as sputtering to rapidly progress. Molecular Dynamics (MD) simulation is one kind of atomistic simulation allows us to simulate gas-solid interaction problems. MD simulation relies on a Newtonian approach of a defined number of atoms' positions of velocities. We use the LAMMPS MD simulator to perform our gas-solid interaction simulations[10]. The purpose of this simulation is to determine the reflection model of xenon ion on solid material. Figure 3 shows the simulation flow chart of LAMMPS. At each time step, the software LAMMPS calculates the new positions and velocities of each atoms according to interaction potentials within a given simulation box. All particle information can be output at any time step, and then the physical parameter such as sputtering yield can be calculated. The input file made by the user must compound every particle property, but also the interaction potentials and other functions precisely defined, such as thermostats.

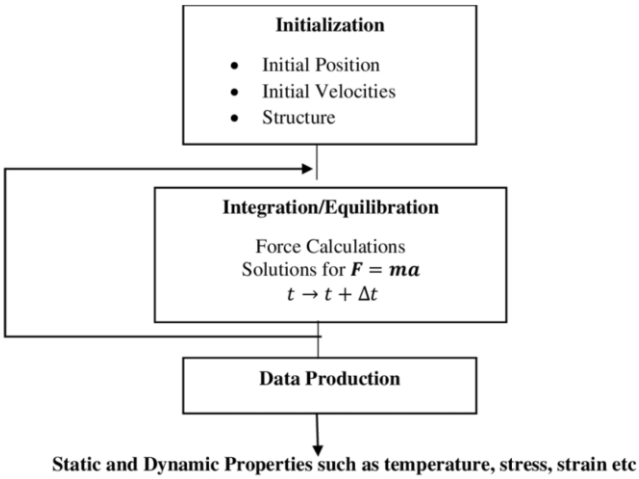

Figure 3. LAMMPS molecular dynamics flowchart.

B. Simulation model

In order to simulate the trajectory of reflected and sputtered atom, two simulation layers are created. The first simulation layer consists of a crystalline metal target formed from a pure element. Here, Aluminum is set to the simulation target because it is often used to the material for beam target installed in space chamber. The incidence plane to is chosen to be the highest density plane of the crystal. The (1 1 1) plane for a Face-Centered Cubic lattice. The metal target was made of 12 × 12 × 8 crystal 3cells, with periodic boundary conditions applied to the x-and y-axis boundaries and free boundary conditions applied to the z-axis boundaries.

Projectile xenon ions are set on another simulation layer made on the top of the crystal. All projectiles have the same kinetic energy and impact the target at a chosen incidence angle. The position and velocity of the reflected or impinging xenon ions are recorded. Interactions between multiple projectiles are ignored.

Two interatomic potentials are required, one between atoms within the target and one between projectile ions and target atoms. The embedded atom method (EAM) potential is used for our simulation. The potential energy between two atoms is given by

$$E_i^{EAM} = F_\alpha\left(\sum_{j\neq i}\rho_\beta(r_{ij})\right) + \frac{1}{2}\sum_{j\neq i}\phi_{\alpha\beta}^{EAM}(r_{ij}). \tag{4}$$

Here, ρ is the atomic electron density used to compute the embedding energy F_α, which represents the energy required to embedded an atom i of type α into the electron cloud of an atom j of type β. The distance r_{ij} is from atom i to atom j and the $\phi_{\alpha\beta}^{EAM}$ is the pair potential between atom of type α and β. The EAM potential is widely used for metal systems since its embedded energy term accounts for multi-body interactions. We used an EAM file developed by Ackland[11].

The Ziegler–Biersak–Littmark (ZBL) universal potential is chosen for the interactions between projectile ions and target atoms[12]. This potential represents screened coulombic repulsion between atomic nuclei. The potential energy between two atoms i and j at a distance r_{ij} is given by

$$E_{ij}^{ZBL} = \frac{1}{4\pi\epsilon_0}\frac{Z_i Z_j e^2}{r_{ij}}\phi^{ZBL}(r_{ij}/a) + S(r_{ij}), \tag{5}$$

where e is the electron charge, Z_i and Z_j are the nuclear charges of the two atoms in electron charge units, and ϵ_0 is the electrical permittivity of a vacuum. The pair potential $\phi^{ZBL}(x)$ and the parameter a is given by the literature. The $S(r_{ij})$ is a switching function that ramps the potential to zero between an inner and outer cutoff distance. This potential is already implemented in LAMMPS, and only needs two parameters: both particles nucleus charge.

The main simulation comprises the initialization of a crystal to a steady state in 5ps, followed by a given number of iterations. The first 1ps step consists of the reflection of one xenon atom on the surface, when the sputtering can occur. The second 1ps step is a refreshing time of the surface in order to get back to a steady state of the surface for the next incident atom. Without this refreshing time, it takes huge time to achieve the surface to be steady state due to the limited simulation crystal size. The Langevin thermostat is used and this thermostat emulates heat conduction into the surrounding material which are not modeled in this simulation. This thermostat is applied to the middle layer constructed by four lattice. The bottom layer constructed by two lattice is fixed to prevent the crystal from shifting[12]. The top four lattice layer is free. It is worth noticing that more than four lattice layer is needed to avoid the thermostat affecting the simulation result with multiple injection more than a thousand.

C. Validation by sputtering yield calculation

Sputtering yield calculation of Xenon-Aluminum was conducted for validation of our LAMMPS code. We put a xenon ion on the upper area of the lattice randomly with normal incident angle. Firstly, the steady state of the sputtering yield was confirmed with multiple injection of 300eV xenon. Figure 4 shows the calculated sputtering yield versus number

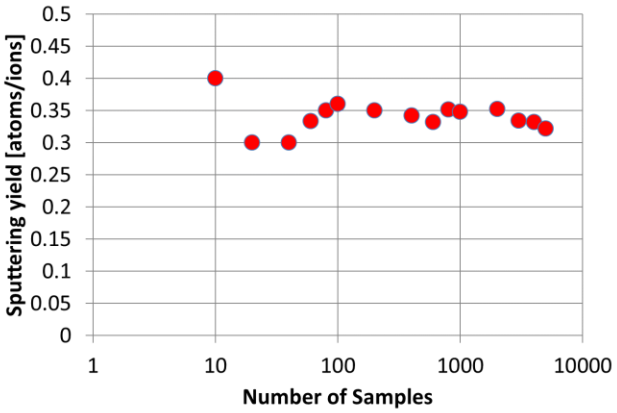

Figure 4. Sputtering yield vs Number of samples.

of samples of injected xenon. Here the sputtering yield is calculated by the ratio of sputtered atoms to injected xenon. The calculated sputtering yields with low samples less than 100 are dispersed and the results with larger samples more than 100 takes almost stable around 0.35. Note that more than 5000 samples, three of four free lattice are sputtered and the sputtering yield become lower than 0.35 due to the effect of thermostat. The history of the sputtered lattice is shown in Fig,5. As summary, the simulation reached to the steady state with more than 100 samples.

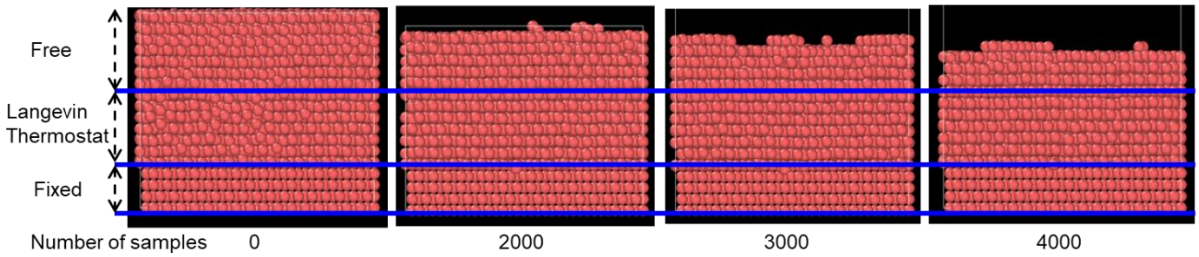

Figure 5. The history of sputtered lattice.

Figure 6 shows the simulated sputtering yield and literature results of different xenon energy. The simulated sputtering yield shows the good agreement with literature results from 300 eV to 800 eV. The discrepancy in low energy and high energy is explained by that ZBL potential is adaptable to the range of few 100 eV. For lower energy like less than 200 eV, combined potential of ZBL and EMA is proposed. Such combined potential is complex and we need to develop it as future work. Nevertheless, between 300 eV to 800 eV, our code successfully simulated the

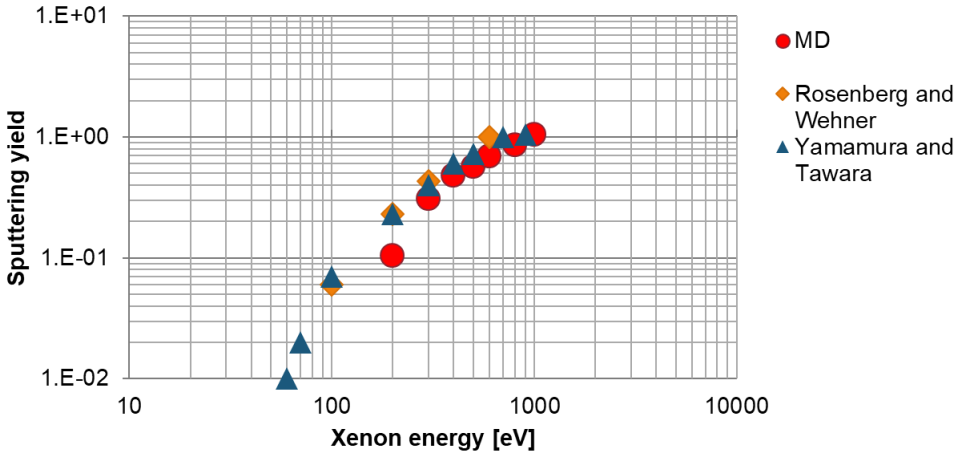

Figure 6. Comparison of simulated (red) and reported sputtering yield[13,14] with 300eV xenon injection at normal incident angle.

gas-solid surface interaction.

D. Simulated wall accommodation property and modeling

The reflected particle trajectory is also calculated. The polar angular distribution of reflected velocity vector is shown in Fig. 7. The result is compared to the Cercignani-Lampis-Lord (CLL) model[15]. The distribution from MD simulation shows closer to the central axis compared to diffusion. The calculated kinetic energy of reflected xenon is distributed around 4eV, as shown in Fig.8. The parameters for CLL model to satisfy both the polar angular distribution and kinetic energy distribution are 0.986 for both accommodation coefficient and 3000 K for reflected temperature. This high temperature means the kinetic energy of incident xenon ion is converted to the internal energy. This result is obtained only by normal incident angle but the incident angular dependency is able to be obtained by this simulation.

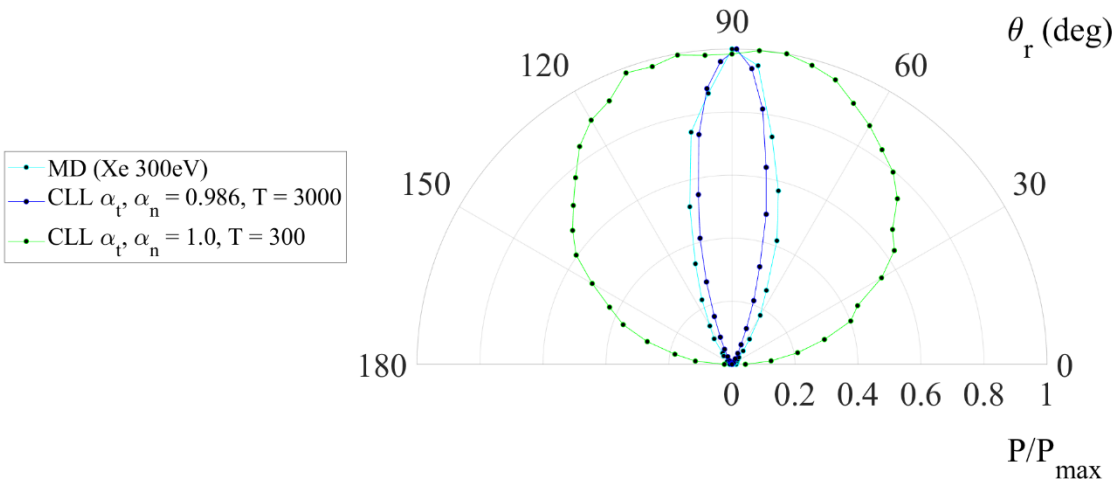

Figure 7. Polar angular distribution of reflected xenon velocity vector.

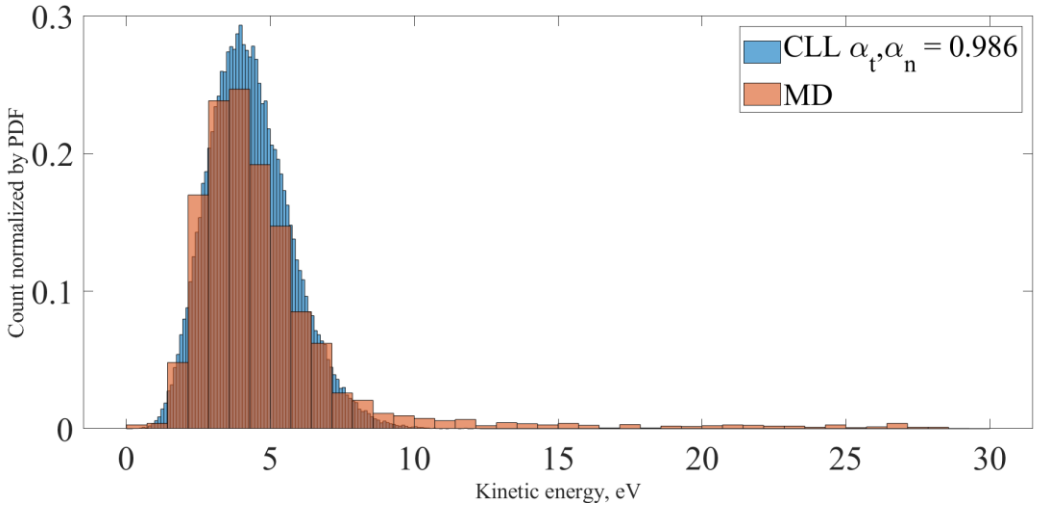

Figure 8. Kinetic energy distribution of reflected xenon.

IV.DSMS simulation for background flux estimation

The DSMC method is a technique for modelling a real gas by directly simulating thousands or millions of molecules. The velocity and position coordinates of these molecules are stored at every time step. Then the calculation at each time step is divided into two procedures: an update of the particle position by the translational motion and an update of the molecular velocity through representative collisions chosen by Monte Carlo sampling and boundary interactions such as diffusion with thermal accommodation in the simulated physical space. The mathematical and theoretical details of the DSMC method are fully described in an earlier report[16].

The schematic of our 2D3V (two-dimensional for position and three-dimensional for velocity) simulation model is shown in Fig.9. Because our target chamber is Ø 2.0 × 3.0 m cylindrical vacuum chamber at IHI, cylindrical coordinated is used. The particle velocity is set to 2.0×10^4 m/s, the velocity of ion accelerated by 275 V which is the measured value during the experiment by using retarding potential analyzer. The velocity vector from point source is given by beam divergence angle with 40 degrees of half-divergence angle. Note that any electromagnetic forces are not calculated in this simulation. When the particles across the chamber wall, particles are reflected obeying wall accommodation model. Here, MD result approximated by CLL model is used for initial particle reflection. For the comparison, complete diffusion case is also calculated. For particle wall reflection after fist

reflection, diffusion model is used based on the assumption that the background xenon particles are captured on the chamber surface not exposed by ion beam and the collision with these particles makes the reflection randomly. The particles which across pump area are deleted from the simulation regarding to pump capture coefficient. Here, average pump capture coefficient 0.55 is used[9]. Only two cryogenic pumps with 30-inch-diameter are installed in the chamber. In order to model this limited pump area, the ratio of pump surface area to the cylindrical surface area of the pump diameter region is multiplied to the pump capture coefficient. the Inter-particle collision was calculated by the Null-Collision method[16]. Cell size for the calculation of the particle collision and macro particle size are determined to keep more than twenty simulated particles inside the cell. Here, mesh number is 60×20 and the macro particle size is 1.0×10^{12}. The variable soft sphere (VSS) model is used. The collision cross section is calculated by following equation reported by Koura[17].

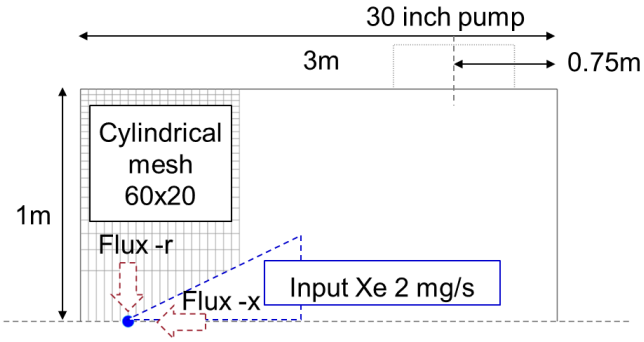

Figure 9. The schematic of 2D3V-DSMC simulation model.

$$\sigma_{VSS}(Xe,Xe) = \frac{2.117\times10^{-18}}{g^{2\omega}} \tag{6}$$

The simulation results are shown in table 1. We counted background flux toward to the beam source (assumed as Hall thruster) both on z-direction and r-direction. Ideally the flux on r-direction stands for the thermal flux because no flux source exists in this axis. If the ratio of flux –z to flux –r is larger, the background flow toward the Hall thruster is generated. The case 1 and two is simple comparison between the effect of wall accommodation model. In both case, the ratio of flux –z and flux –r is close to one. This means that the background flow can be considered to be thermalized flow condition. Because of multiple reflection before the particles reach to the upstream region, particles lose their energy and directionality observed in the first reflection. In addition, due to the downstream pump, background particle which is thermalized by multiple reflection is dominant around the upstream region. This is the reason why the mean velocities of z-direction are almost zero. In order to clarify the effect of pump location, the simulation with upstream pump location cases are conducted. The pump center is located 0.75 m downstream from the chamber upstream end (assumed to be opposite Hall thruster position). The simulation results are listed as case 3 and 4 in the table 1. Even with the diffusion reflection, the mean velocity and ratio of flux slightly increase due to the pump location effect. However, the difference between the MD accommodation model and diffusion model case is still small. The reason is considered to be the limitation of pump area. In the case 5 and 6, we increase

Table 1. Simulation results of 2D3D-DSMC.

Case	accommodation model	pump position	pump surface ratio	mean -v_x, m\s	Flux -z, /s/m^2	Flux -r, /s/m^2	ratio fo flux z/r
1	MD	down	0.0242	0.10	2.16E+19	2.09E+19	1.03
2	Diffusive	down	0.0242	0.64	1.93E+19	1.92E+19	1.00
3	MD	up	0.0242	-1.42	2.09E+19	2.09E+19	1.00
4	Diffusive	up	0.0242	-1.98	2.05E+19	1.92E+19	1.07
5	MD	up	0.2540	-10.69	4.94E+18	3.13E+18	1.58
6	Diffusive	up	0.2540	-9.59	4.07E+18	2.91E+18	1.40

the pump area by considering whole cylindrical region of the area pump located are occupied by pumps. As a result, the ratio of flux –z to flux –r and mean flow velocity are increased and the difference between the MD accommodation model and diffusion model is clearly seen. This suggests that the effect of wall accommodation on the background flux increases in the case of Hall thruster operation at the facility with large upstream pump capacity.

V.Conclusion

The facility background pressure effect was observed in the experiment of the 1kW-class SPT-type Hall thruster. The estimated background flux $1.74 \times 10^{20}\ /s/m^2$. is 4.8 times larger than the thermal flux estimated with the measured pressure. The calculated background flux by one-dimensional background flow model is $3.66 \times 10^{20}\ /s/m^2$ and this is similar to the thermal flux. This implies that some improvement of the model is needed to evaluate the background flow property.

The wall reflection model is the key factor to reproduce the background flow experiment in particle simulation. The MD simulation code to calculate gas-solid surface interaction based on LAMMPS software was developed and validated by sputtering yield calculation. From 300eV to 800eV, this code successfully reproduced the sputtering yield of xenon-aluminum. The calculated polar angular distribution of reflected xenon was compared to the CLL wall accommodation model and it was shown that the simulated distribution is closer to the specular like reflection compared to diffusion. In addition, the reflected particles keep kinetic energy around 4eV. In order to implement obtained wall accommodation model to the DSMC simulation, the parameters for CLL model to satisfy both the polar angular distribution and kinetic energy distribution are estimated by approximation, and these are 0.986 for both accommodation coefficient and 3000 K for reflected temperature.

The background flux was calculated by 2D3V-DSMC simulation and the wall accommodation model dependency was studied. When pumps are located only in downstream region, the effect of wall accommodation model can be negligible to the background flux due to energy loss by the multiple wall reflection. On the other hand, the effect of the wall accommodation model becomes larger when the pumps are located on the upstream and they have higher pumping capacity. In order to achieve low background flux and low mean flow velocity, downstream pump location is suitable. This study implies that downstream pumps with limited pumping capacity, the background flux becomes same value as thermal flux. In order to estimate the quantity of the performance change due to the background pressure effect, the study of the way how and where ingestion particles are ionized is necessary.

Acknowledgments

The authors would like to thank researchers from IHI corporation and Mr. Hugo Sapin (*Ecole Centrale de Lyon, France*) who provided insight and expertise that greatly assisted the research part of molecular dynamics simulation.

References

[1] Funaki, I., S. Iihara, S. Cho, K. Kubota, H. Watanabe, K. Fuchigami, and Y. Tashiro, "Laboratory Testing of Hall Thrusters for All-Electric Propulsion Satellite and Deep Space Explorers," *52nd AIAA/SAE/ASEE Joint Propulsion Conference, 2016*, American Institute of Aeronautics and Astronautics, Reston, Virginia, 07/25/2016.

[2] Hamada, Y., J. Bak, R. Kawashima, H. Koizumi, K. Komurasaki, N. Yamamoto, Y. Egawa, I. Funaki, S. Iihara, S. Cho, K. Kubota, H. Watanabe, K. Fuchigami, Y. Tashiro, Y. Takahata, T. Kakuma, Y. Furukubo, and H. Tahara, "Hall Thruster Development for Japanese Space Propulsion Programs," *Transactions of JSASS*, Vol. 60, No. 5, 2017, pp. 320–326.

[3] Randolph, T., V. Kim, H. Kaufman, K. Kozubsky, V. Zhurin, and M. Day, "Facility Effects on Stationary Plasma Thruster Testing," *23rd International Electric Propulsion Conference*, Seattle, USA, 1993.

[4] Hofer, R.R., and J.R. Anderson, "Finite Pressure Effects in Magnetically Shielded Hall Thrusters," *50th AIAA/ASME/SAE/ASEE Joint Propulsion Conference*, American Institute of Aeronautics and Astronautics, Reston, Virginia, 07/28/2014.

[5] Diamant, K.D., R. Liang, and R.L. Corey, "The Effect of Background Pressure on SPT-100 Hall Thruster Performance," *50th AIAA/ASME/SAE/ASEE Joint Propulsion Conference*, American Institute of Aeronautics and Astronautics, Reston, Virginia, 07/28/2014.

[6] Cai, C., I.D. Boyd, and Q. Sun, "Free Molecular Background Flow in a Vacuum Chamber Equipped with Two-Sided Pumps," *Journal of Vacuum Science & Technology A Journal of Applied Physics Journal of Applied Physics*, Vol. 24, No. 115, 2006, pp. 11101–203304.

[7] Cho, S., H. Watanabe, K. Kubota, S. Iihara, K. Honda, K. Fuchigami, K. Uematsu, and I. Funaki, "Parametric Kinetic Simulation of an IHI High Specific Impulse SPT-Type Hall Thruster," *50th AIAA/ASME/SAE/ASEE Joint Propulsion Conference*, American Institute of Aeronautics and Astronautics, Reston, Virginia, 07/28/2014.

[8] Frieman, J.D., T.M. Liu, and M.L.R. Walker, "Background Flow Model of Hall Thruster Neutral Ingestion," *Journal of Propulsion and Power*, Vol. 33, No. 5, 2017, pp. 1087–1101.

[9] Ito, G., R. Kawashima, K. Komurasaki, and H. Koizumi, "Inflow Angular Dependence of the Capture Coefficient in Cryopumps," *Vacuum*, Vol. 160, February 2019, pp. 102–108.

[10]Large-scale Atomic/Molecular Massively Parallel Simulator, LAMMPS, http://lammps.sandia.gov(accessed 08/15/2019).

[11] Winey, J. M., Alison Kubota, and Y. M. Gupta, "A Thermodynamic Approach to Determine Accurate Potentials for Molecular Dynamics Simulations: Thermoelastic Response of Aluminum," *Modelling and Simulation in Materials Science and Engineering*, Vol. 17, No. 5, 2009.

[12] Wise, E.S., M.S. Liu, and T. Miller, "Sputtering of Cubic Metal Crystals by Low-Energy Xenon-Ions," *Computational Materials Science*, Vol. 107, 2015, pp. 102–109.

[13] Rosenberg, D., and G. K. Wehner, "Sputtering Yields for Low Energy He+-, Kr+-, and Xe+-Ion Bombardment," *Journal of Applied Physics*, Vol. 35, No. 5, 1962, pp.1842-1845.

[14] Yamamura, Yasunori, and Hiro Tawara, "'Energy Dependence of Ion-Induced Sputtering Yields from Monatomic Solids at Normal Incidence," *Atomic Data and Nuclear Data Tables*, Vol. 62, No. 2, 1996, pp.149-253.

[15] Lord, R.G., "Some Extensions to the Cercignani-Lampis Gas-Surface Scattering Kernel," *Physics of Fluids A*, 1991.

[16] Bird, G.A., *Molecular Gas Dynamics and the Direct Simulation of Gas Flows* Oxford Univ. Press, New York, 1994.

[17] Koura, K., and H. Matsumoto, "Variable Soft Sphere Molecular Model for Inverse-power-law or Lennard-Jones Potential," *Physics of Fluids A: Fluid Dynamics*, Vol. 3, No. 10, October 1991, pp. 2459–2465.